Surface Soil Moisture Estimates from AMSR-E Observations over an Arid Area, Northwest China

Lei Wang[1], Jun Wen[1*], Tangtang Zhang[1], Yizhou Zhao[2], Hui Tian[1], Xiaokang Shi[1],Xin Wang[1], Rong Liu[1], Jinhui Zhang[1], Shaoning Lu[1].

[1]. Key Laboratory for Climate-Environment and Disasters of Western China, Cold and Arid Regions Environmental and Engineering Research Institute, Chinese Academy of Sciences, Lanzhou, Gansu 730000, China

[2]. Xinjiang Climate Center, Urumqi, Xinjiang 830002, China

*Correspondence to: PhD. Lei WANG, No. 320 Donggang West Road, Lanzhou Gansu 730000, China. Cold and Arid Regions Environmental and Engineering Research Institute, Chinese Academy of Sciences. Tel: 0086-931-4967076 (O), Fax: 0086-931-4967109, E-mail: lwang@lzb.ac.cn

Abstract

In this paper, 7 years (during the growing season (April-October) of 2002-2008) of the Advanced Microwave Scanning Radiometer for the Earth Observing System (AMSR-E) data taken at a frequency of 6.9 GHz for night observations at both polarizations are processed and used to obtain 7 years of surface soil moisture dataset for an arid area, in northwestern China. This soil moisture dataset can contribute to better understanding the climate change and forecast modeling for this area. Based on the first-order radiative transfer model calculation, a unique model for estimating surface soil moisture over the study area is developed. Considering extremely complex topography over the study area, we present a parameterization of surface roughness at the 6.9 GHz and spatial resolution of the AMSR-E using the annual minimum MPDI (Microwave Polarization Difference Index). For validation, the comparisons of soil moisture patterns with precipitation fields are made. The results indicate the evolution of soil moisture estimated from the developed model and antecedent ground daily precipitations are in a good agreement. Comparisons of the estimated values of soil moisture with the ground observations are also made for two representative sites over 2002-2004. The results indicate there is a good agreement between them, with higher correlation coefficients (R=0.649, 0.604) and RMSE (3.5, 5.4%), and the soil moisture product derived from the AMSR-E is realistic and acceptable. This new long time series of the estimated soil moisture will prove valuable for other studies of climate change and model evaluation.

1 Introduction

Surface soil moisture is a key variable of water and energy exchanges at the land surface/atmosphere interface and thus has potential applications in hydrology, meteorology, and climate change studies. For climate applications, soil moisture is considered as the most important indicator of the effect of increase in greenhouse gases on the climate (Rowntree and Bolton, 1983). Real-time soil moisture measurements are vital for crop monitoring and drought warning. Previous research has shown that passive microwave remote sensing sensors can be used to monitor soil moisture over land surfaces (Choudhury and Golus, 1988; Paloscia et al., 1993; Drusch et al., 2001; Jackson, 1993; Lakshmi et al., 1997; Njoku et al., 2005; Owe et al., 2008). Investigations have established the fundamentals of passive microwave remote sensing for monitoring temporal and spatial variations of regional soil moisture (Kerr and Njoku, 1990; Mo et al., 1982). Ground-based soil moisture network can not be built reasonably without consideration of huge cost. However, satellite observations are available in real-time and provide good temporal and spatial coverage. The effects of vegetation cover and surface roughness play a significant role in the microwave emission from the surface (Jackson and Schmugge, 1991; Njoku and Chan, 2006). Therefore, good parameterization schemes of these two effects are prerequisite for retrieving surface soil moisture information. Low frequencies are preferable for soil moisture estimates since perturbing factors such as atmospheric moisture, vegetation canopy, and surface roughness are less significant (Ulaby et al., 1982; Choudhury et al., 1979). Consequently, recent advances in science and technology have resulted in space agency commitments to L-band (1.4 GHz) missions in the near future (Kerr, 2001; Kerr et al., 2007). There are several microwave

radiometers operating in space now (Jackson et al., 2005). Though their frequencies are higher than L-band, they have potential for estimating surface soil moisture in regions with low level of vegetation. The Advanced Microwave Scanning Radiometer for the Earth Observing System (AMSR-E) is one of them. In the current investigation, an alternative retrieval technique utilizing the AMSR-E 6.9 GHz observations and based upon the work of Njoku and Li (2003) is implemented and tested for an arid area.

Some typical techniques available for the estimation of surface soil moisture from the passive microwave observations are given below.

1.1 Single channel algorithm

Several significant examples of this algorithm have been performed by Jackson et al. (Jackson, 1993; Jackson et al., 1995; Jackson and Le Vine, 1996; Jackson et al., 1999), which are based on the radiative transfer equation and use a channel that is most sensitive to soil moisture. This algorithm uses volumetric Vegetation Water Content (VWC) approximating the optical depth and incorporates soil texture, surface roughness and temperature using *h*-polarized brightness temperature, and is then used with a dielectric model to obtain the soil moisture.

1.2 Multichannel iterative algorithm

This approach is successfully used for AMSR-E estimates to carry out three parameters simultaneously: surface soil moisture, soil temperature and vegetation water content (Jackson, 1993; Njoku and Li, 1999; Njoku et al., 2003). However unanticipated Radio Frequency Interference (RFI) problem is encountered at the 6.9 GHz frequency (Njoku et al., 2005; Li et al., 2004), requiring modification of this

approach. A radiative transfer model, the ω-τ model, is used for this algorithm. First, the higher frequencies in terms of 18 and 37 GHz are used for surface classification. Next, the ω-τ model is employed in comparing with measured and computed brightness temperatures at four channels (6.9 and 10.7 GHz, dual polarization). Finally, the three parameters are obtained until the difference between the computed and observed brightness temperatures is minimized in a least squares sense. The principal of this algorithm is to discriminate between the three parameters considering the sensitivity differences between horizontal (H) and vertical (V) polarizations, and between frequencies.

1.3 Polarization index algorithm

Owe et al. (2001, 2008) has shown the potential of this algorithm for developing a historical climatology of continuous satellite-derived global land surface soil moisture. The Microwave Polarization Difference Index (MPDI) can effectively eliminate or minimize the effects of surface temperature. This algorithm uses a nonlinear iterative procedure in a forward modeling approach to separate the surface emission from the vegetation emission, and then optimizes on the vegetation optical depth and the soil dielectric constant. Once convergence between the computed and the observed brightness temperatures is achieved, the model uses a global database of soil physical properties together with a soil dielectric mixing model to solve for the surface soil moisture.

Arid and semi-arid land accounts for 40% of the earth's surface. From climatological, ecological and anthropogenic perspectives, the spatio-temporal distributions of soil moisture over arid and semi-arid land are very important. Nowadays, climate change in arid areas is one of the main focuses in global warming

which the international community is most concerned about. Desertification and arid ecosystem deterioration induced by arid climate variation and their impacts on the natural environment and anthropogenic activities have been given priority in recent years.

An arid region in northwestern China, Xinjiang, is focused on in this paper. Our research into microwave land surface soil moisture for the study area here has been motivated by a need to better understanding the climate change and forecast modeling for this area. The study area is also interesting because of diversity of its surface types and complexity of its topography. So far, no such attempt has been made exclusively for this region from literatures.

The existing models for estimating soil moisture need more ancillary parameters. Among them, the model developed by Owe et al. (2001, 2008) need least ancillary parameters. A key to their Land Parameter Retrieval Model (LPRM) is deriving surface temperature using from 37 GHz vertical polarization brightness temperature observations. However, Owe et al. indicated that deriving daytime surface temperature was a significant problem in arid and semiarid locations because of more intense surface heating. In our practice, the "significant problem" occurs heavily over the study area, even during night time. Thus we attempt to develop a specialized model for monitoring soil moisture over the study area.

2 Study area and data descriptions

2.1 Description of study area

The Xinjiang Uygur Autonomous Region of China is located in the hinterland of the Eurasian continent. Lying in northwestern China (Fig. 1), Xinjiang covers a huge area of 1,660,000 km^2 with 49.5% mountains, 28% plains and 22.5% deserts, occupying

one-sixth of China's total territorial area and larger than any other Chinese province or autonomous region.

The Xinjiang region is characterized by its unique topography with an extremely large elevation range from -154 m in the Turfan Basin to 8611 m at the summit of Qiaogeli. The Altay and Kunlun Mountain ranges lie in the north and the south of Xinjiang, respectively. The magnificent Tianshan Mountain, with an elevation of 3000 to 5000 m, stretches from east to west in the middle of the region, dividing Xinjiang into north and south sections. The Junggar Basin between the Tianshan and the Altay ranges contains the Gurbantunggut Desert in the middle. The Tarim Basin is enclosed by the Tianshan and the Kunlun ranges with the Taklimakan Desert in the middle.

Due to its unique geography, this area has a conspicuous continental arid climate, with large diurnal temperature range, abundant sunshine, very large potential evaporation and low precipitation. It has annual average temperatures of 4.1-7.8 ºC and 10.2-12.3 ºC for the north and the south of Xinjiang, respectively. The rainfall is concentrated mainly in the summer season, with annual precipitation of about 146 mm.

2.2 Description of datasets

2.2.1 AMSR-E brightness temperature observations

In this paper, the AMSR-E brightness temperature (TB) observations are employed for estimating soil moisture. The AMSR-E instruments onboard the EOS/Aqua platform have been a component of the Defense Meteorological Satellite Program since June, 2002. The AMSR-E instruments are a conical scanning total power microwave radiometer system operating at a constant incidence angle of 54.8° across a 1445-km swath at six frequencies: 6.9, 10.7, 18.7, 23.8, 36.5, and 89 GHz. All the

channels operate in both V and H polarization. Spatial resolution ranges from approximately 60 km at 6.9 GHz to 5 km at 89 GHz. The orbital period is about 102 min, which results in 14.1 orbits per day. For a given satellite, coverage is possible twice a day approximately 12 hr apart on the ascending and descending passes. The orbit is sun-synchronous with equator crossings at about 01:30 and 13:30 LT. Additional information can be found in Njoku et al. (2003).

The AMSR-E measurements used here are AMSR-E/Aqua Daily Girded Brightness Temperatures available at the National Snow and Ice Data Center (NSIDC) (Knowles, 2006). They are in the north EASE-Grid projection, with all channels having 25 km resolution and equidistant latitude-longitude projection at 0.25° resolution.

The 2002-2008 daily rain-gauge data from 95 meteorological stations operating in Xinjiang are used for validations. The data are available from the Xinjiang Climate Center of China. The stations, however, are most installed in the well-populated zones on the front plains of the mountains and the outskirts of the deserts (Fig. 1).

2.2.2 Ground soil moisture observations

For further validation, we take advantage of soil moisture observations, consisting of 2 stations (Altay (88.08°E, 47.73°N) and Shache (77.27°E, 38.43°N)) in the study area, for the period 2002-2004, to evaluate the estimated soil moisture from the AMSR-E. These observations were taken using the gravimetric technique for each 10-cm layer down to a depth of 0.5 m. The data were observed three times a month on the 8, 18 and 28th days, generally for the growing season (April to October). The data were originally recorded as percent wetness by mass of dry soil. Using soil density information available for each layer at each site, we determined the volumetric soil moisture. Only the data of the top layer (0-10 cm) are used for comparison purpose.

2.2.3 Ground rainfall observations

The 2002-2008 daily rain-gauge data from 95 metrological stations operating in Xinjiang are also used for validations. The data are available from the Xinjiang Climate Center of China. The stations, however, are most installed in the well-populated zones on the front plains of the mountains and the outskirts of the deserts (Fig. 1). Among of them, six representative stations—Tazhong (83.67°E, 39.00°N), Mosuowan (86.10°E, 45.02°N), Yutian (81.65°E, 36.85°N), Altay (88.08°E, 47.73°N), Qinghe (90.38°E, 46.67°N), and Hetian (79.93°E, 36.85°N) (see Fig. 4)，were selected according to the consistency of their classifications of land use in 2000 with those using the subsequent MPDI method. The first three locations represent bare soil condition, particularly Tazhong just lying in the center of the Taklimakan Desert. The others represent vegetated soil condition.

2.2.4 Soil properties

The dielectric mixing model developed by Hallikainen et al. (1985) is used to convert volumetric soil moisture (VSM) into soil dielectric constant. This mixing model requires percent of sand and clay as inputs, in addition to VSM. A 1-degree resolution global soil texture dataset (Webb et al., 1991) is used (http://daac.ornl.gov/). This dataset consist of 2 files. One file contains the depth and particle size (percent sand, silt, and clay) information for each major continent, soil type, and soil horizon. The other file contains ocean/continental coding and Zobler soil type classifications (Zobler, 1986).

2.2.5 Land use classification map

For the study, WESTDC_Land_Cover_Products1.0, the 1-km land use map, from Environmental & Ecological Science Data Center for West China (http://westdc.westgis.ac.cn) is used to validate the result of classifying vegetation and bare soil using the MPDI. This data follow Resource and Environment Classification System of Chinese Academy of Sciences. The groups include cropland, forest, grassland, permanent glacier and snow, water body, urban and built-up and unused land. To be compatible to the AMSR-E resolution (25-km), the 1-km land use map was resampled to an EASE-Grid 25-km resolution (Fig. 4).

2.2.6 ERA-interim daily volumetric soil water

Alternative data for validation in the study are atmospheric model interim_daily Surface Analysis ERA Interim Volumetric soil water layer 1, obtained from the ECMWF data server. They are at 1.5° resolution, with time coverage 2002-2008, soil depth is corresponding to 7 cm. Because the water content is standardized to the 7 cm depth of the top layer, to convert soil water content to volumetric soil moisture is just divided by 0.07.

Additionally, soil moisture can not be estimated under snow cover or frozen soil conditions because the soil moisture dependence on the dielectric constant become small when surface soil temperature is below 0 ℃ (Hallikainen et al., 1985). Therefore, days with snow cover or frozen soil are eliminated from the present study. The period from the beginning of April to the end of October is, in general, historically free-frozen and snow-free for entire study area except for mountains. Thus, this period is taken into account for analysis, and hereinafter referred as to an “annual cycle”.

3 Theoretical background and methodology

Passive microwave remote sensing is based on the measurement of thermal radiation from the land surface in the centimeter wave band. This radiation is largely determined by two components: physical temperature and emissivity of the underlying radiating body. Many land parameters have distinct properties that affect microwave emissivity in various ways. Dielectric properties and surface roughness may describe the properties.

The approach for this paper is based on the first-order radiative transfer theory. The influence of atmospheric moisture and the multiple scattering in the vegetation layer are assumed to be neglected. Furthermore, if the soil and vegetation temperatures are approximately equal and represented by a single surface temperature T_S (K), the primary relationship between surface parameters and microwave brightness temperatures T_b can be expressed (Kerr and Wigneron, 1995; Njoku et al., 2003; Mo et al., 1982):

$$T_{bp} = T_S\{e_{sp}\Gamma_p + (1-\omega_p)(1-\Gamma_p)[1+(1-e_{sp})\Gamma_p]\} \quad (1)$$

where ω is single scattering albedo of the vegetation, and the subscript p is polarization of the measurement, H or V, e_s is emissivity of the soil surface which is related to the reflectivity r_s by：

$$e_{sp} = 1 - r_{sp} \quad (2)$$

The transmissivity (Γ) of the vegetation and can be expressed as a function of the vegetation opacity along the observation path:

$$\Gamma_p = \exp(-\tau_{cp}/\cos\theta) \quad (3)$$

where θ is the incidence angle, τ_c is the vegetation opacity along the observation path which could be linearly related to the total VWC using the so called b_P parameter

(Jackson and Schmugge, 1991):

$$\tau_{cp} = b_p VWC \tag{4}$$

The investigators have shown that the use of lower frequencies results in far less canopy attenuation of the soil emission. At lower frequencies, a value 0.15 of the parameter for *b* is appropriate for most agriculture crops. Methods for estimating the VWC have also been developed by passive microwave remote sensing. Investigators have explored relationships between the MPDI and vegetation parameters for a given vegetation type (Paloscia et al., 2001; Wen et al., 2005; Choudhury and Tucker, 1987).

The soil reflectivity at a given incidence angle is mainly related to soil moisture through the complex permittivity of the soil (Wang and Schmugge, 1980; Dobson et al., 1985). However, in general, surface roughness also affects the surface reflectivity because of scattering. To account for soil roughness, the *h*-*Q* formulation (Wang et al., 1983) is often used, and then the reflectivity of a rough surface, r_{sp}, is related to that of an equivalent smooth surface, r_{op}, as follows:

$$r_{sp} = [(1-Q)r_{op} + Qr_{oq}]\exp(-h) \tag{5}$$

where *p* and *q* denote orthogonal polarizations. The surface roughness parameter *h* is proportional to the quantity $(ks)^2$, where *k* is the wave number ($k = 2\pi/\lambda$) and *s* is standard deviation of the surface height (cm). The parameter *Q* contains information on both the vertical and the horizontal roughness correlation length, *l*.

The MPDI is defined as:

$$MPDI = \frac{T_{bV} - T_{bH}}{T_{bV} + T_{bH}} \tag{6}$$

The MPDI is frequently used to minimize or eliminate the effects of variable surface temperature dependence, leading to a close relationship to the dielectric properties of the emitting surfaces. The MPDI decreases with increasing vegetation

water content because denser vegetation usually depolarizes the soil emission. For bare soil, the MPDI decreases with decreasing soil moisture because the soil emission is less polarized when the free water content in the soil is reduced.

For clarity, the theoretical relationship between the MPDI and the vegetation optical depth is simulated with the radiative equation (Fig. 2). For bare soil, Fig. 2(a) shows the MPDI increases nonlinearly with increasing soil moisture, while for vegetated soil MPDI has a more complex relationship to soil moisture. The two effects of soil moisture and vegetation water content on the MPDI are synergistic in general. The MPDI decreases when vegetation water content increases and/or soil moisture decreases. When vegetation water content increases the MPDI sensitivity to soil moisture decreases rapidly. Additionally, when MPDI is less than 0.01 or the vegetation optical depth is approximately greater than 0.8, the information of soil moisture is attenuated by high vegetation biomass and therefore can not be derived. Additionally, Fig. 2(b) depicts the relationship between the MPDI and the vegetation optical depth for a range of surface roughness. The two effects of surface roughness and vegetation water content on the MPDI are also interactive. It can be seen that sensitivity of the MPDI to soil moisture decreases nonlinearly very rapidly with surface roughness. This nonlinear attenuation effect of surface roughness is very similar to that of vegetation water content. Therefore, some investigators combined the two effects into one parameter to conduct temporal dynamics of vegetation water content (Njoku and Chan, 2006) and surface soil moisture (Jin and Yan, 2007).

3.1 Parameterization of vegetation opacity

In this study, we use a numerical solution for the vegetation optical depth developed by Meesters at al. (2005) instead of using ancillary data or other surrogates (e.g. *NDVI*

and *LAI*). Using a retrieval methodology, the optical depth is derived from the MPDI and the dielectric constant of the soil, which improves the accuracy and overall efficiency of the soil moisture estimates.

From Meesters at al., the numerical solution for the vegetation optical depth is:

$$\tau = \cos\theta \ln(ad + \sqrt{(ad)^2 + a + 1}) \tag{7}$$

Then, according to Eq. (3)

$$\Gamma = \frac{1}{ad + \sqrt{(ad)^2 + a + 1}} \tag{8}$$

where a and d are defined as

$$a = 0.5(\frac{e_V - e_H}{MPDI} - e_V - e_H) \tag{9}$$

and

$$d = \frac{\omega}{2(1-\omega)} \tag{10}$$

The assumption that the vegetation single scattering has minimal effect on emissivity is widely accepted (Jackson et al., 1982). For simplification, we neglect the effect of the single scattering. Thus, for an incidence angle, the vegetation opacity is ultimately expressed a function of the MPDI, the soil emissivity which highly related to soil dielectric properties and the surface roughness. So, if the surface roughness is known, the vegetation opacity can be obtained by an interactive method related to the MPDI, soil moisture, and its soil texture information.

3.2 Parameterization of Surface Roughness

Parameterization of the surface roughness is a key problem in this paper. First, we rewrite (6) by Eq. (1), (7)-(10) as:

$$MPDI = \frac{e_V - e_H}{e_V + e_H}(1-2Q)\{1 + \frac{2}{e_V + e_H}[\exp(2\tau + h) - 1]\}^{-1} \tag{11}$$

This equation can be rework to the expression of the combined surface parameters of the surface roughness and the vegetation opacity, using Eq. (5):

$$\tau + 2h = \cos\theta \ln[0.5 * (1 - 2Q)(r_{Ho} - r_{Vo})MPDI^{-1} + r_{Ho} + r_{Vo}] \quad (12)$$

In Eq. (11), besides soil moisture, there are only two parameters unknown: the two parameters of surface roughness. Note that the vegetation opacity can be solved by the method described in the above section. Thus，if the values of surface roughness corresponding to Q and h are available, we can readily estimate the soil moisture. However, the ancillary data of surface roughness are sparse. For lower frequency (at 1.4 GHz), Q would have a minimum effect on the surface moisture calculations, while h is usually set with a lower value. Some investigators usually use a fixed value for roughness parameterization and assume the remainder of roughness can be automatically coupled with the vegetation effects (Owe et al., 2001; Njoku et al., 2003; Owe et al., 2008). Generally, when surface roughness conditions are unknown, a value of zero is often assigned to Q, and a value between 0 and 0.3 is typically assumed for h (Jackson, 1993). At the 6.9 GHz frequency, Njoku and Chan (2006) used Q as a fixed global calibration factor leaving h to incorporate the roughness spatial variability. For the desert region in Saudi Arabia, with a global minimal topographic variation, a value of Q (0.174) was adopted as a fixed parameter to calibrate the AMSR-E data globally to the microwave model for a baseline minimum roughness level, assuming h=0.

The challenge for us is to separate these variables from the emitting signal by using a minimum of ancillary data. Apart from the brightness temperature data, we have only the ancillary data of soil texture. As previously mentioned, the study area is characterized by its extremely complex topography. Assuming the value of Q assigned as 0.174, if the value of h was assigned a fixed value (e.g., 0.2), the soil moisture estimates could not be made for many places of this study area except for desert regions. The reason for this explanation is that the uniform value of surface

roughness is probably much lower for the regions of complex topography. We have therefore realized using a uniform value of h for entire area is not reasonable.

As there are minimal human activities over the study area, the roughness is practically less disturbed for the AMSR-E footprint size, so it could have a fairly invariant distribution with long time. First, we assumed the roughness is unchanging during an annual cycle. We further supposed the driest soil to have ~5.5% volumetric soil moisture. The later assumption was probably somewhat higher for desert regions while lower for other regions. Note that the penetration depth at 6.9 GHz is only approximately 1.0-2.0 cm (Jackson and Schmugge, 1989). There are no soil moisture measurements in this depth, although, it is self-evident that the soil moisture at this depth is in general lower than that at deeper depth (e.g. 5cm). Njoku et al. (2006) speculated the value of VSM in dry soil condition in the desert region of Al-Hadidah is round 5.0%.

For bare surface, the minimal VSM corresponds to the minimal MPDI (MPDImin) from the AMSR-E observed over an annual cycle. Wang et al. (2006) found the MPDI could be used to roughly classify the vegetation and bare soil by analyzing the MPDI at 6.9GHz in 5 experiment fields in China, 2003, and the data of land use. They concluded the threshold for distinguishing between vegetated and bare soil surfaces using the MPDI was about 0.04 at 6.9 GHz. We assumed the values of the VSM for the driest bare soil in this study area are slight higher than that in region of Al-Hadidah, thus 5.5% was a reasonable value of volumetric soil moisture in driest surface soil condition. This baseline minimum value was used ultimately to compute h at each footprint for bare soil ($MPDI_{min}$ >0.04). As a consequence, total footprints for bare soil account for 62.3% in this study area. The others involved vegetated soil, frozen soil, snow cover, glacier etc. Fig. 3 is the map of the $MPDI_{min}$ for 2005.

Compared to the map of land use (Fig. 4), the regions of vegetated/bear soil distinguished by MPDI are more continuous. This may be closer to the reality of the land cover for 2005. The accuracy of interpretation at the vegetated/bare soil level is satisfactory since this simple MPDI classification method makes the correct interpretation 87.8%.

Ignoring a very few abnormal negative values, the areas corresponding to the $MPDI_{min}$ not greater than 0.01 may be the glaciers lying on the mountains of Tianshan and Kunlun mountain. The areas corresponding to the $MPDI_{min}$ ranging from 0.01 to 0.02 are usually characterized by perennial snow covers on mountains or some dense forests. As for the areas corresponding to the $MPDI_{min}$ ranging from 0.02 to 0.04, they indicate the ever presence of vegetation. Note throughout this paper that the areas ranging from 0.02 to 0.04 only indicate that there were covered by vegetations all the time or just at times. That is to say, there were less vegetations or bare soils covering the same areas at some or even long time for a given annual cycle.

Figure 5 shows the map of the h parameter in 2005 over the study area derived by Eq. 12. All the h patterns for other years are almost the same as this one. Note that the lower values of h correspond to the areas of dry, flat, and comparably homogeneous soil conditions, especially the Taklimakan Desert and the Gurbantunggut Desert.

The maximum value of h in bare soil areas is 0.73 and higher values of h mostly exist in the transition zones between deserts and mountains (purple color) where are characterized by great gradients of DEM. Except for the regions of glacier, perennial snow and dense forest ($MPDI_{min}<0.02$), the no-bare regions are most the transition belts between mountains and deserts where are particularly rugged. Thus, considering large areas of high mountain where soil moisture can not be estimated due to glacier, perennial snow and dense forest covers (even though given a normal h value, the soil

moisture can not be retrieved there), the *h* value is set to 0.6. We tested the *h* values ranging from 0.2 to 1.3 for the no-bare region for deriving soil moisture, and the value 0.6 for *h* was empirically appropriate.

4 Algorithm implementation, results and validations

4.1 Implementation

The previously described methodology has been applied to the historical dataset of nighttime AMSR-E brightness temperatures for the study area. A 7-year time series of estimated daily soil moisture dataset was obtained. Considering the greater stability of nighttime surface temperatures, only nighttime data were used in the study. Additionally, days with snow cover or frozen soil were also eliminated from the analysis, and therefore we just have selected the growing season (April to October).

An iterative procedure was developed for the forward radiative transfer model that iteratively computes the simulated MPDI for VSM ranging from 5.5% to 45%, in 0.1 % increments. The single-scattering albedo of the vegetation was set as 0.0 for both H and V polarization. At each iteration step, for 6.9 GHz, the computed MPDI values were compared to the satellite observations. If the absolute value of the differences between the computed and observed MPDI was less than 0.0015, then the input soil moisture would be saved in array. During the iteration process, the dielectric mixing model developed by Hallikainen et al. (1985) was used to convert VSM into soil dielectric constant. This mixing model requires percent of sand and clay as input, in addition to VSM. The soil texture classification of the surface soil on a 1-degree grid for this study area was used here (Webb et al., 1991).

4.2 Results

4.2.1 Mean annual soil moisture patterns

Figure 6 depicts the 7-year estimated mean annual soil moisture patterns. In general, the mean annual soil moisture is around 9%. The lower values exist in desert regions especially in the Taklimakan Desert, and higher values are present on northeastern Kunlun Mountain and in the transition zones between deserts and mountains, where are drainage regions. Significantly, the glaciers and/or snow covers distributed on the tops of mountains are automatically computed as no-value regions where the convergence between the calculated and the observed MPDI was no longer achieved because of the extremely low MPDI resulting from depolarization prosperities of glaciers and snow covers.

To further explore the dynamic characteristics of soil moisture, the year 2005 was selected for this investigation.

4.2.2 Annual maximum soil moisture pattern

For arid areas, actually, annual maximum soil moisture pattern reflects the soil moisture information resulting from a maximum (or accumulative) precipitation in a (or a series of) rainfall event(s). From Fig. 7, there are three obvious characteristics: 1) The desert regions (both the Taklimakan Desert and the Gurbantunggut Desert) are characterized by higher soil moisture values. For the Taklimakan Desert, the maximum soil moisture range is from 25% to 30% and for the Gurbantunggut Desert, the maximum soil moisture is 25-40%. Another area of higher soil moisture values shows on northeastern Kunlun Mountain with values ranging of 30-40%. 2) The eastern part of the study area is characterized by low values with ranging of 6-8%,

meaning little chance and few rainfall events took place in this region. 3) On the transition zones between mountains and deserts are apparently high values, probably resulting from topographic effects on large precipitations.

4.2.3 Typical rainfall traces captured

There are comparatively sparse meteorological stations in the huge area, although, a series of typical rainfall events were found (Fig. 8). The events occurred on August 4-6, 2005 (DOY of 216-218), which were characterized in the IR images by a long belt of frontal cloud crossing the study area from north to south. High estimated soil moisture conditions were captured during the rainfall period. The frontal system traveled the Taklimakan Desert from west to east , producing light to moderate rainfall. Dry conditions (10% VSM) prevailed at the beginning of the rainfall events over the Taklimakan Desert. During the rainfall period, The Taklimakan Desert shows a series of rainfall traces with three sequential center regions of increased soil moisture conditions. The maximum values of estimated soil moisture reaches 22.0%, 29.2 % and 37.8% for these three center regions, respectively. Note that the soil moisture conditions in these regions became rapidly dry after these meteorological events.

4.3 Validations

We validate surface soil moisture products from the AMSR-E because the model for estimating soil moisture by utilizing formulations and with assumed or parameterized parameters have not been or are even impossible to be thoroughly developed and verified. Many of these procedures have been qualitative in nature. These limitations must result in uncertainties on the accuracy of the estimated surface soil moisture.

However, there are no reliable and spatially averaged ground-measured surface

moisture measurements for validation purposes, especially at the satellite scale. In addition, although ground measurements are precise, each of them represent at only a specific point and hence can not be used to calculate the mean that the large satellite field of view (FOV) can accomplish, unless they are densely measured. we compare the AMSR-E estimates of VSM and ground observations for two representative sites, the Altay site and Shache site, on the 8, 18 and 28th days over 2002-2004. Comparison with precipitation fields is often a validation option available. Although this method can not validate the estimated soil moisture quantitatively, it can at least provide qualitative trend information. To do this, we selected 6 meteorological stations for point validation. For each of the locations, matches between estimated soil moistures and antecedent measured daily precipitations were made. Moreover, ERA-interim daily volumetric soil water field was applied to validate, though the results is not satisfactory.

4.3.1 Comparison with in situ observations

Validation of the soil moisture retrieval algorithm here is based on comparisons of the AMSR-E estimates of VSM and ground observations for two sites, the Altay site and Shache site, on the 8, 18 and 28th days over 2002-2004. Fig. 9 shows comparisons of measured soil moisture with the estimated soil moisture for the two sites. Generally, the estimated soil moisture has temporal scale comparable to observations, but has small amplitude of variation. This small amplitude can be attributed to low sensitivity of soil moisture at FOV scale compared to that at point scale. In spite of some dispersion in data, higher correlation coefficients (R=0.649, 0.604 for the two sites, respectively) and RMSE (3.5, 5.4%) are shown in Table 1. we can conclude that the algorithm is quite able to estimate the correct value of VSM. Fig. 10 shows plots of

estimated verse measured soil moisture for the two sites. Generally, the algorithm overestimates the soil moisture amount on the dry condition (below 14%) and, on the contrary, underestimates the soil moisture amount on the wet condition (above 14%), with positive average differences on the order of 2 %.

These results clearly demonstrate that the estimated VSM from the AMSR-E is consistent with the ground observations and strongly supports the developed retrieval algorithm.

4.3.2 Temporal variability of estimated soil moisture

Six stations were selected as the representatives for different surface types (vegetated surface, desert surface, bare arid surface) and climatic characteristics (the north and the south climate, separately). Figure 11 shows time series of estimated VSM and antecedent observed precipitation in 2005 for six representative locations—Tazhong, Mosuowan Yutian, Altay, Qinghe, and Hetian. In general, the temporal patterns of precipitation and soil moisture for both bare and vegetated soil condition are characteristically coincident. It can be seen that Tazhong is mostly associated with extremely low soil moisture condition (5.5% VSM) except for the rainy days when soil moisture increases up sensitively and afterwards decreases to original lever quickly. This must be a result of very high evaporative demand in this region. Mosuowan, Yutian show the characteristic behavior of soil moisture where it also increases up responding to rainfall event evidently. Soil moistures at Altay, Qinghe, and Hetian also response to rainfall event evidently. However, they show high dispersions compared to the locations of bare soil. Highly variable surface temperature could be responsible for this reason. After rainfall event, soil moisture gradually decreases. This lag is largely attributed to the retention capacity of soil

moisture of vegetated soil.

4.3.3 Comparison with ERA-interim daily volumetric soil water

To be compatible to the ERA-interim product, the estimated soil moisture from the AMSR-E was resampled to a 1.5° resolution. Unfortunately, we found the ERA-interim daily volumetric soil moistures varied little over the study area. Here, we present the comparisons of the AMSR-E soil moisture with the ERA-interim soil moisture for only three locations in 2004. The three location are Altay, Shache, and Tazhong lightened in Fig. 4. From Fig. 12, the ERA-interim product loses its strength over the study area, maintaining a low lever with low dispersion compared to the AMSR-E product. We have not understood why the ERA-interim product over the study area has such behavior. This needs our further investigation. However, from the above section, the AMSR-E product is more convincing.

5 Conclusion and discussions

A model for estimating surface soil moisture over the arid area of Xinjiang, northwest China, from the AMSR-E brightness temperatures at 6.9 GHz was developed. This model was based on first-order radiative transfer model calculation and applied to conduct 7-year period (2002–2008) of soil moisture dataset. We compared the estimated moisture soil with the measured precipitation. Results clearly demonstrated the performance of the model for soil moisture estimates in the study area. The temporal patterns of rainfall and soil moisture for either bare or vegetated soil condition were characteristically coincident and soil moisture also responded to rainfall event evidently, especially for bare soil condition. Furthermore, we captured a series of rainfall traces over the Taklimakan Desert. To quantitatively analysis the

accuracy of the product derived from the AMSR-E, comparisons of the estimated soil moisture with the ground observations were also made for two representative sites. The results indicated the estimated soil moisture followed well this ground observations at temporal scale. Moreover, higher correlation coefficients (R=0.649, 0.604) were obtained, indicating there has a good agreement between them and the soil moisture product derived from the AMSR-E is realistic and acceptable.

Two important model parameters were calibrated a priori. One was vegetation optical depth which was calibrated using an excellent numerical solution which made it possible to separate the effects of surface roughness and vegetation over the vegetated soil regions. The other was surface roughness which was fine-tuned with elaborate assumptions for bare soil and vegetated soil, respectively. The later is worth further discussing as follows.

Surface roughness parameterization is needed prior to surface soil moisture estimates, particularly in complex topographic region. We have supposed the soil moisture corresponds 5.5% for the driest bare soil. Additionally, for vegetated soil, we empirically assigned the parameter h with a uniform value 0.6. These assumptions allow possible and even reliable h parameterization, which has not been possible until now in this study area. However, these guesses would be not right for some footprints. On the other hand, the previous assumption of a value of zero for the single scattering for various vegetations is also unrealistic. In practice, to some extent, the higher assigned h value can offset the effect of underestimation of the single scattering, and then improve the quality of soil moisture estimates.

In addition, the assumed minimum value of 5.5% VSM, for example, must be some higher for some desert soils. ~ 3% may be a realistic guess. However, this input could lead to a negative h value. Volume scatting can account for this issue. This uncertainty

in the *h* parameterization will propagate into the retrieval algorithm as part of the soil moisture biases, although, the present study shows progress in the characterization of the surface roughness, and proves potential for surface moisture estimates.

Moreover, the model is mathematically well behaved, so convergence is normally fast and the glaciers and/or snow covers distributed on the tops of mountains can be computed as no-value regions automatically. The estimated soil moisture dataset now has been made available for climate analysis and forecast modeling for the study area.

References

Choudhury, B. J., Schmugge, T. J., Chang, A. T., and Newton, R. W.: Effect of surface roughness on the microwave emission from soils. Journal of Geophysical Research, 84, 5699-5706, 1979.

Choudhury, B. J., and Tucker, C. J.: Monitoring global vegetation using Nimbus-7 37 GHz Data Some empirical relations, International Journal of Remote Sensing, 8, 1085-1090, 1987.

Choudhury, B. J., and Golus, R.: Estimating soil wetness using satellite data, International Journal of Remote Sensing, 9, 1251-1257, 1988.

Dobson, M., Ulaby, F., Hallikainen, M., and El-Rayes, M.: Microwave Dielectric Behavior of Wet Soil-Part II: Dielectric Mixing Models, Geoscience and Remote Sensing, IEEE Transactions on, 23, 35-46, 1985.

Drusch, M., Wood, E., and Jackson, T.: Vegetative and Atmospheric Corrections for the Soil Moisture Retrieval from Passive Microwave Remote Sensing Data: Results from the Southern Great Plains Hydrology Experiment 1997, Journal of Hydrometeorology, 2, 181-192, 2001.

Hallikainen, M. T., Ulaby, F. T., Dobson, M. C., and El-Rayes, M. A.: Microwave Dielectric Behavior of Wet Soil-Part 1: Empirical Models and Experimental Observations, Geoscience and Remote Sensing, IEEE Transactions on, 23, 25-34, 1985.

Jackson, T., Schmugge, T., and Wang, J.: Passive Microwave Sensing of Soil Moisture Under Vegetation Canopies, Water Resources Research, 18, 1137-1142, 1982.

Jackson, T., and Schmugge, T.: Passive microwave remote sensing system for soil moisture: some supporting research, Geoscience and Remote Sensing, IEEE Transactions on, 27, 225-235, 1989.

Jackson, T., and Schmugge, T.: Vegetation effects on the microwave emission of soils, Remote Sensing of Environment, 36, 203-212, 1991.

Jackson, T..: Measuring surface soil moisture using passive microwave remote sensing, Hydrological Processes, 7, 139-152, 1993.

Jackson, T., Le Vine, D., Swift, C., Schmugge, T., and Schiebe, F.: Large area mapping of soil moisture using the ESTAR passive microwave radiometer in Washita'92, Remote Sensing of Environment, 54, 27-37, 1995.

Jackson, T., and Le Vine, D.: Mapping surface soil moisture using an aircraft-based passive microwave instrument: algorithm and example, Journal of Hydrology, 184, 85-99, 1996.

Jackson, T., Le Vine, D., Hsu, A., Oldak, A., Starks, P., Swift, C., Isham, J., and Haken, M.: Soil moisture mapping at regional scales using microwaveradiometry: the Southern Great Plains Hydrology Experiment, Geoscience and Remote Sensing, IEEE Transactions on, 37, 2136-2151, 1999.

Jackson, T., Bindlish, R., Gasiewski, A., Stankov, B, Klein, M. Njoku, E, Bosch, D, Coleman, T, Laymon, C, Starks, P.: Polarimetric scanning radiometer C- and X-band microwave observations during SMEX03, Geoscience and Remote Sensing,

IEEE Transactions on, 43, 2418- 2430, 2005.

Jin, Y., and Yan, F.: A change detection algorithm for terrain surface moisture mapping based on multi-year passive microwave remote sensing (Examples of SSM/I and TMI Channels), Hydrological Processes, 21, 1918-1924, 2007.

Kerr, Y. H., and Njoku, E. G.: A semiempirical model for interpreting microwave emission fromsemiarid land surfaces as seen from space, Geoscience and Remote Sensing, IEEE Transactions on, 28, 384-393, 1990.

Kerr, Y. H., and Wigneron, J. P.: Vegetation models and observations—A review, in: Passive Microwave Remote Sensing of Land-Atmosphere Interactions, edited by: Pampaloni, B. T. C., Y.H. Kerr and E.G. Njoku, VSP, The Netherlands, 28, 1995.

Kerr, Y. H., Waldteufel, P., Wigneron, J. P., Martinuzzi, J., Font, J., and Berger, M.: Soil moisture retrieval from space: the Soil Moisture and OceanSalinity (SMOS) mission, Geoscience and Remote Sensing, IEEE Transactions on, 39, 1729-1735, 2001.

Knowles, K. W., M. H. Savoie, R. L. Armstrong, and M. J. Brodzik.: updated current year. AMSR-E/Aqua daily EASE-Grid brightness temperatures, 2005. Boulder, Colorado USA: National Snow and Ice Data Center. Digital media, 2006

Kerr, Y. H.: Soil moisture from space: Where are we? , Hydrogeology Journal, 15, 117-120, 2007.

Lakshmi, V., Wood, E., and Choudhury, B.: Evaluation of Special Sensor Microwave/Imager Satellite Data for Regional Soil Moisture Estimation over the Red River Basin, Journal of Applied Meteorology, 36, 1309-1328, 1997.

Li, L., Njoku, E., Im, E., Chang, P., and Germain, K.: A preliminary survey of radio-frequency interference over the US in Aqua AMSR-E data, Geoscience and Remote Sensing, IEEE Transactions on, 42, 380-390, 2004.

Meesters, A., De Jeu, R., and Owe, M.: Analytical derivation of the vegetation optical depth from the microwave polarization difference index, Geoscience and Remote Sensing Letters, IEEE, 2, 121-123, 2005.

Mo, T., B. J. Choudhury, Schmugge, T. J., and Jackson, T. J.: A model for microwave emission from vegetation-covered fields, Journal of Geophysical Research, 87, 1229-1237, 1982.

Njoku, E. G., and Li, L.: Retrieval of land surface parameters using passive microwave measurements at 6-18 GHz, Geoscience and Remote Sensing, IEEE Transactions on, 37, 79-93, 1999.

Njoku, E. G., Jackson, T. J., Lakshmi, V., Chan, T. K., and Nghiem, S. V.: Soil moisture retrieval from AMSR-E, Geoscience and Remote Sensing, IEEE Transactions on, 41, 215-229, 2003.

Njoku, E. G., Ashcroft, P., and Chan, T. K.: Global survey and statistics of radio-frequency interference in AMSR-E land observations, Geoscience and Remote Sensing, IEEE Transactions on, 43, 938-947, 2005.

Njoku, E., and Chan, S.: Vegetation and surface roughness effects on AMSR-E land observations, Remote Sensing of Environment, 100, 190-199, 2006.

Owe, M., de Jeu, R., Walker, J., Branch, H. S., Center, N., and Greenbelt, M. D.: A methodology for surface soil moisture and vegetation opticaldepth retrieval using the microwave polarization difference index, Geoscience and Remote Sensing, IEEE Transactions on, 39, 1643-1654, 2001.

Owe, M., de Jeu, R., and Holmes, T.: Multi-Sensor Historical Climatology of Satellite-Derived Global Land Surface Moisture, Journal of Geophysical Research, 113, F01002, doi:10.1029/2007JF000769,2008.

Paloscia, S., Pampaloni, P., Chiarantini, L., Coppo, P., Gagliani, S., and Luzi, G.: Multifrequency passive microwave remote sensing of soil moisture and roughness, International Journal of Remote Sensing, 14, 467-483, 1993.

Paloscia, S., Macelloni, G., Santi, E., and Koike, T.: A multifrequency algorithm for the retrieval of soil moisture on alarge scale using microwave data from SMMR and SSM/I satellites, Geoscience and Remote Sensing, IEEE Transactions on, 39, 1655-1661, 2001.

Rowntree, P. R., and Bolton, J. A.: Simulation of the atmospheric response to soil moisture anomalies over Europe, Quarterly Journal of the Royal Meteorological Society,109, 501-526 1983.

Ulaby, F. T., Moore, R. K., and Fung, A. K.: Microwave remote sensing -active and passive. vol. I: Microwave remote sensing fundamentals and radiometry. Artech House, Boston (MA), USA, 1982.

Wang, J., and Schmugge, T.: An Empirical Model for the Complex Dielectric Permittivity of Soils as a Function of Water Content, Geoscience and Remote Sensing, IEEE Transactions on, 18, 288-295, 1980.

Wang, J., O'Neill, P., Jackson, T., and Engman, E.: Multifrequency Measurements of the Effects of Soil Moisture, Soil Texture, And Surface Roughness, Geoscience and Remote Sensing, IEEE Transactions on, 21, 44-51, 1983.

Wang, L., Li, Z., and Quan, C.: Soil moisture retrieval with AMSR-E in the region with vegetation coverage, High Technology Letters, 16, 204-209, 2006. (In Chinese)

Webb, R., Rosenzweig, C., Levine, E., Aeronautics, U. S. N., Scientific, S. A., and Program, T. I.: A Global Data set of Soil Particle Size Properties, National Aeronautics and Space Administration, Office of Management, Scientific and Technical Information Program, 1991.

Wen, J., Jackson, T., Bindlish, R., Hsu, A., and Su, Z.: Retrieval of Soil Moisture and Vegetation Water Content Using SSM/I Data over a Corn and Soybean Region, Journal of Hydrometeorology, 6, 854-863, 2005.

Zobler, L. 1986. A World Soil File for Global Climate Modelling. NASA Technical Memorandum 87802. NASA Goddard Institute for Space Studies, New York, New York, U.S.A.

Figure captions

Fig. 1. Map of the study area combined with digital elevation model (DEM) and distribution of the meteorological obviation network.

Fig. 2. Theoretical relationship between the MPDI and the vegetation optical depth ,(a) a range of soil dielectric constants (Q=0.174, h=0, and ω=0) ,(b) surface roughness (Q=0.174, *h*=0, and k=12).

Fig. 3. Distribution of the calculated minimal MPDI for 2005.

Fig. 4. Map of the land use, Xinjiang, 2000. Color points represent the locations for validation (1: Altay, 2: Qinghe, 3: Mosuowan, 4: Shache, 5: Hetian, 6: Yutian and 7: Tazhong).

Fig. 5. Distribution of the estimated *h* parameter for 2005.

Fig. 6. Patterns of annual mean surface soil moisture estimated from the AMSR-E at night orbit for years from 2002 to 2008.

Fig. 7. Map of maximum surface soil moisture for year of 2005.

Fig. 8. Dynamics of surface soil moisture resulting from a series rainfall events during 216 to 218 of 2005.

Fig. 9. Time series of estimated VSM corresponding to on the 8, 18 and 28th days (Beijing Time) for the growing season (April to October) from 189 of 2002 through 2008. Left is for the Altay site and right is for Shache site.

Fig. 10. Estimated VSM versus measured VSM for the Altay site (left) and the Shache site (right) over 2002-2004. The black line represents the 1:1 line and the red one represents the fit line.

Fig. 11. Comparisons of estimated soil moisture and measured precipitation at six representative locations. Left are representative to bare soil condition (from top to bottom, corresponding to locations Tazhong, Qinghe, Shache, and right to vegetated soil condition for Yutian, Hetian, and Mosuowan.

Fig. 12. Comparisons of estimated soil moisture and ERA-interim volumetric soil moisture at 3 locations for the growing season (April to October) of 2004.

Table caption

Table 1. Statistics of estimated and measured VSM for the Shache site and the Altay site over 2002-2004.

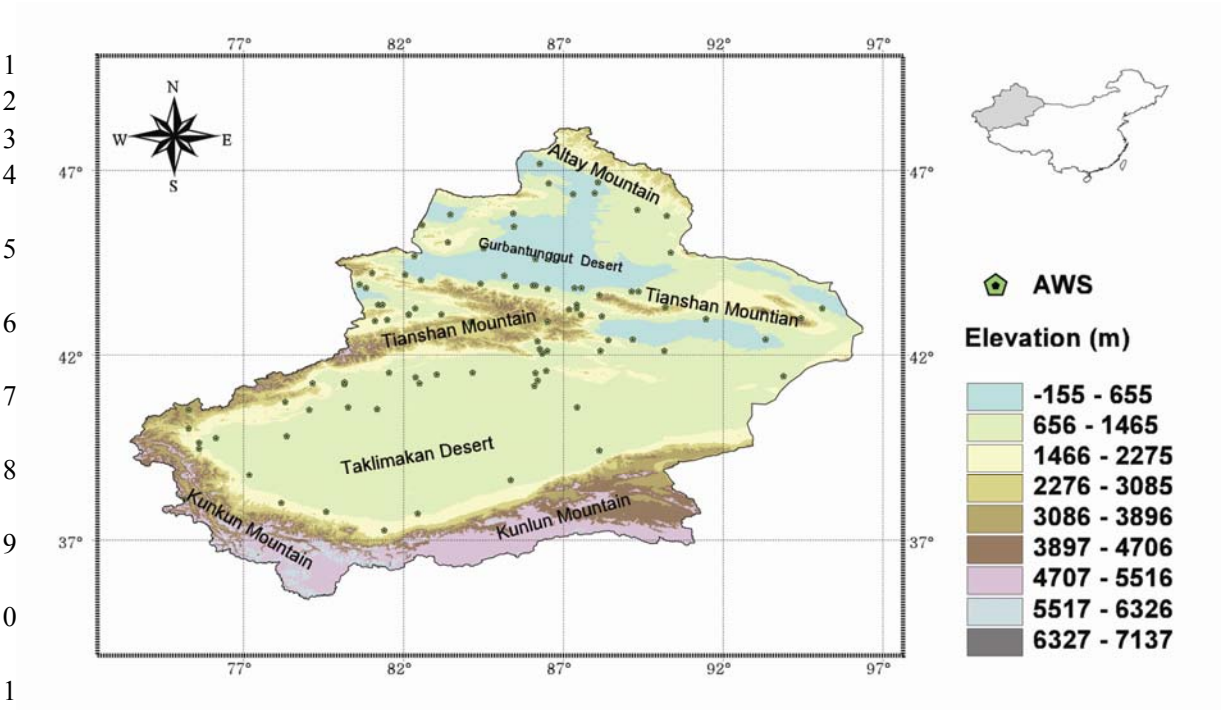

Fig. 1. Map of the study area combined with digital elevation model (DEM) and distribution of the meteorological observation network.

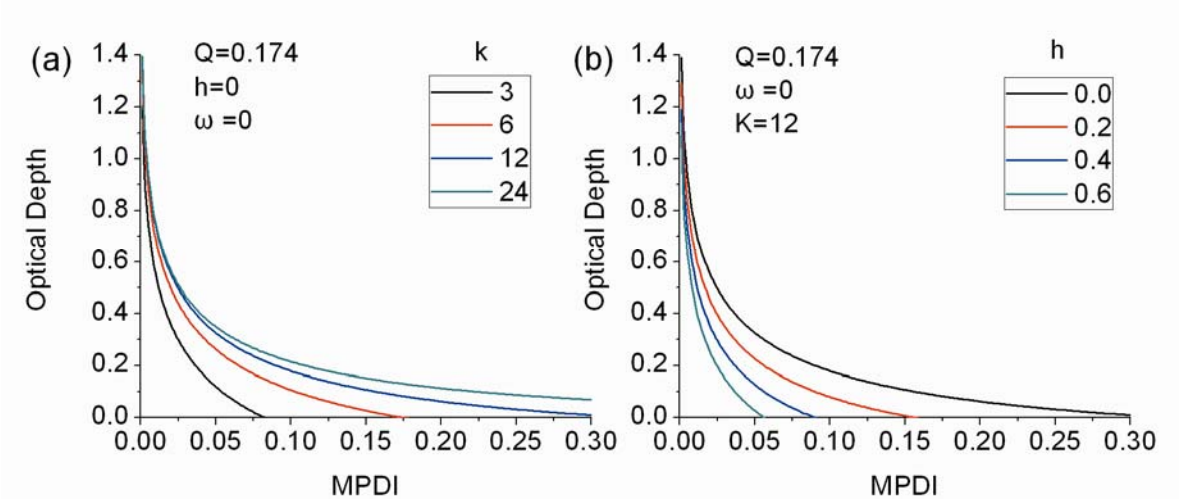

Fig. 2. Theoretical relationship between MPDI and vegetation optical depth ,(a) a range of soil dielectric constants (Q=0.174, h=0, and ω=0) ,(b) surface roughness (Q=0.174, h=0, and k=12).

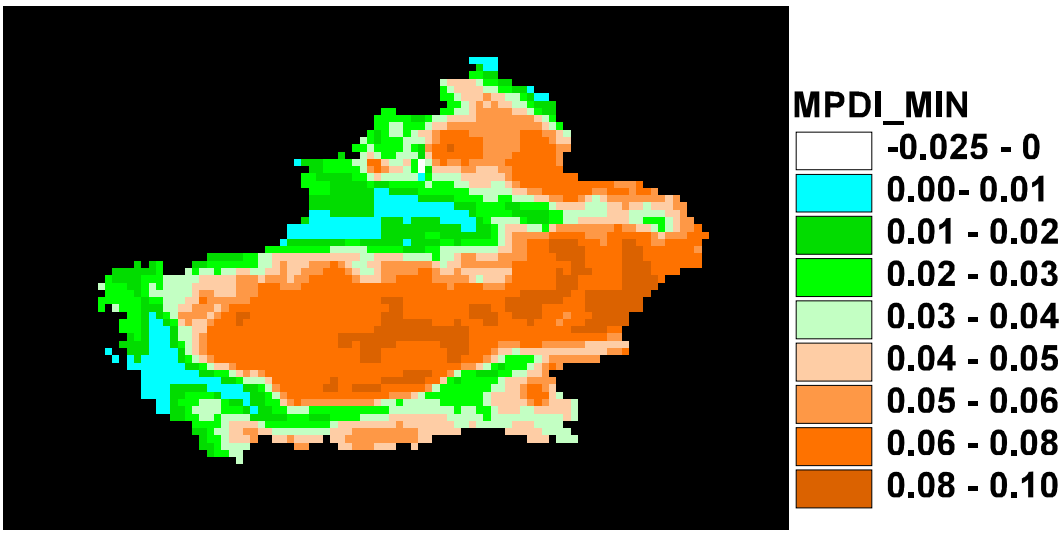

Fig. 3. Distribution of the calculated minimal MPDI for 2005.

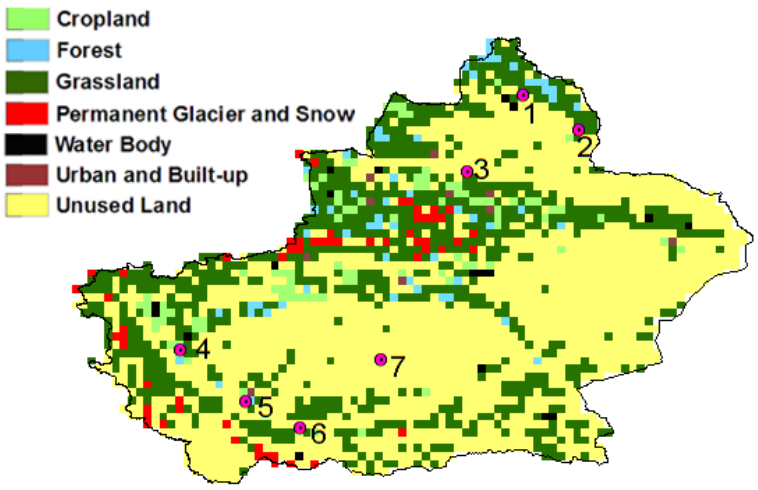

Fig. 4. Map of the land use, Xinjiang, 2000. Color points represent the locations for validation (1: Altay, 2: Qinghe, 3: Mosuowan, 4: Shache, 5: Hetian, 6: Yutian and 7: Tazhong).

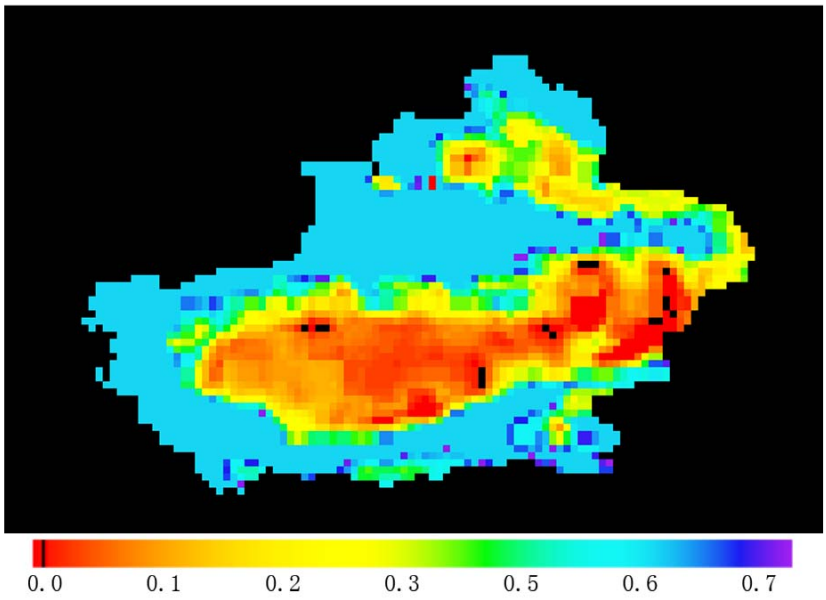

Fig. 5. Distribution of the estimated *h* parameter for 2005.

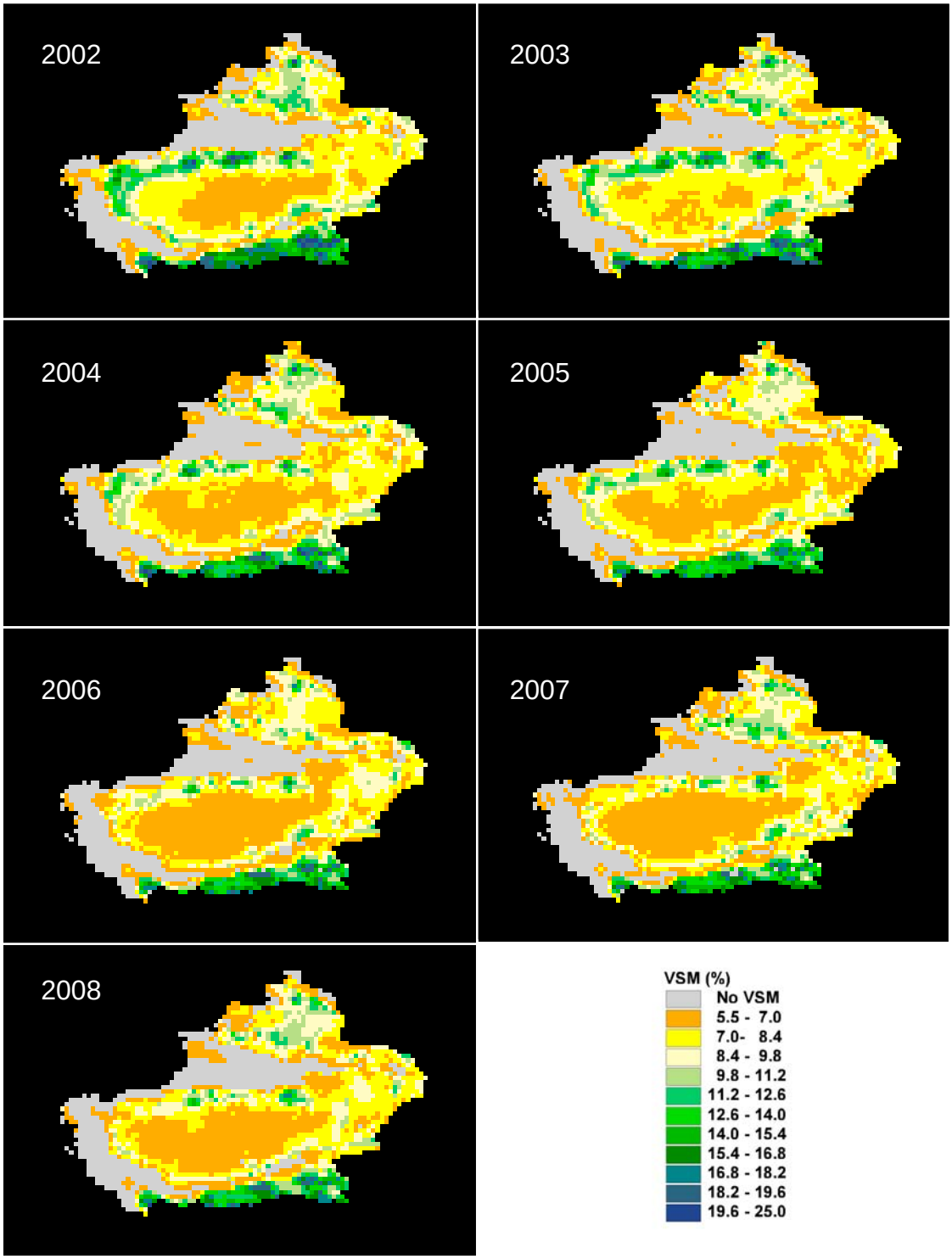

Fig. 6. Patterns of annual mean surface soil moisture estimated from the AMSR-E at night orbit for years from 2002 to 2008

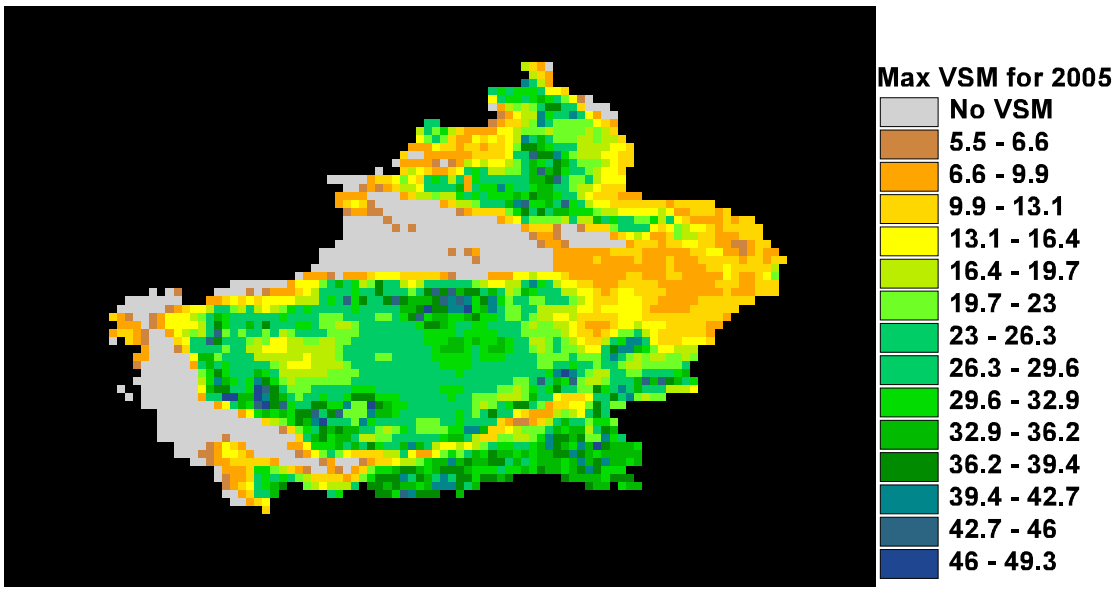

Fig. 7. Map of maximum surface soil moisture for year of 2005.

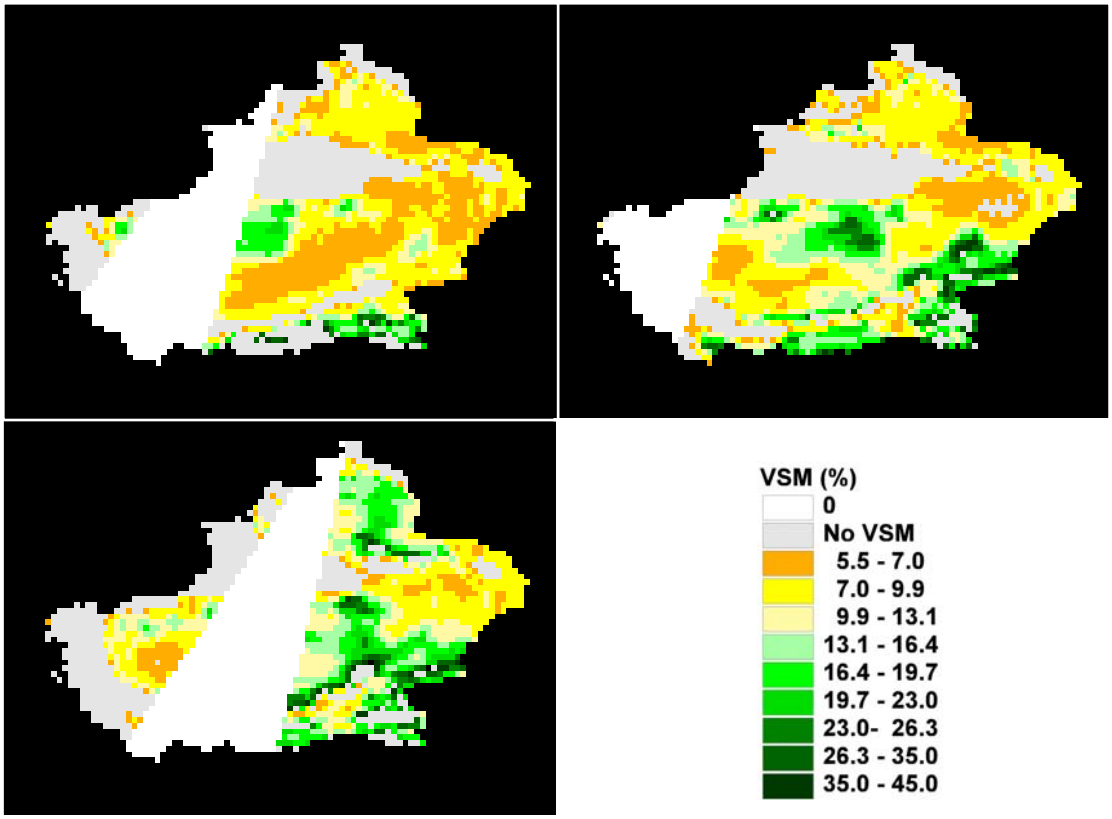

Fig. 8. Dynamics of surface soil moisture resulting from a series rainfall events during 216 to 218 of 2005 (from left to right).

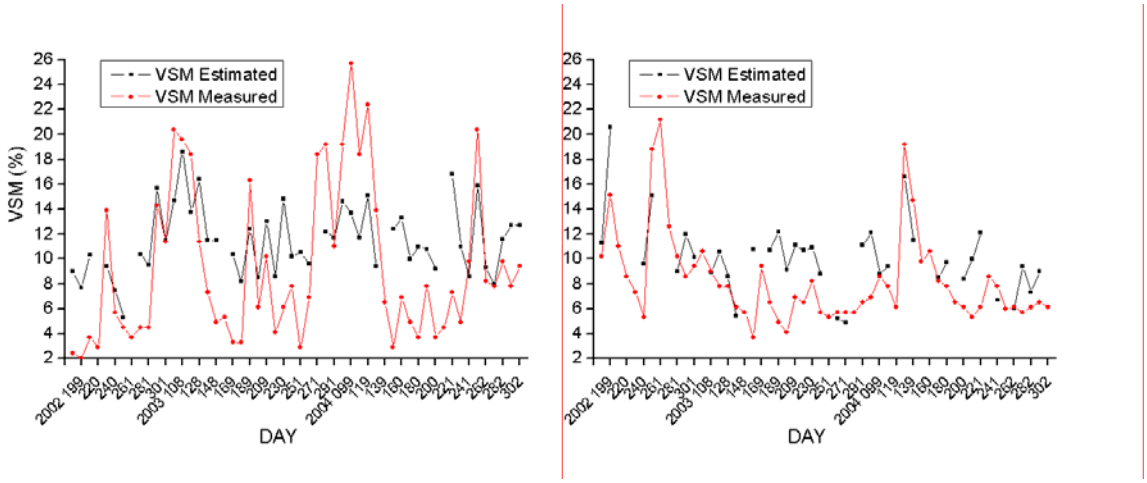

Fig. 9. Time series of estimated VSM corresponding to on the 8, 18 and 28th days (Beijing Time) for the growing season (April to October) from 189 of 2002 through 2008. Left is for the Altay site and right is for Shache site.

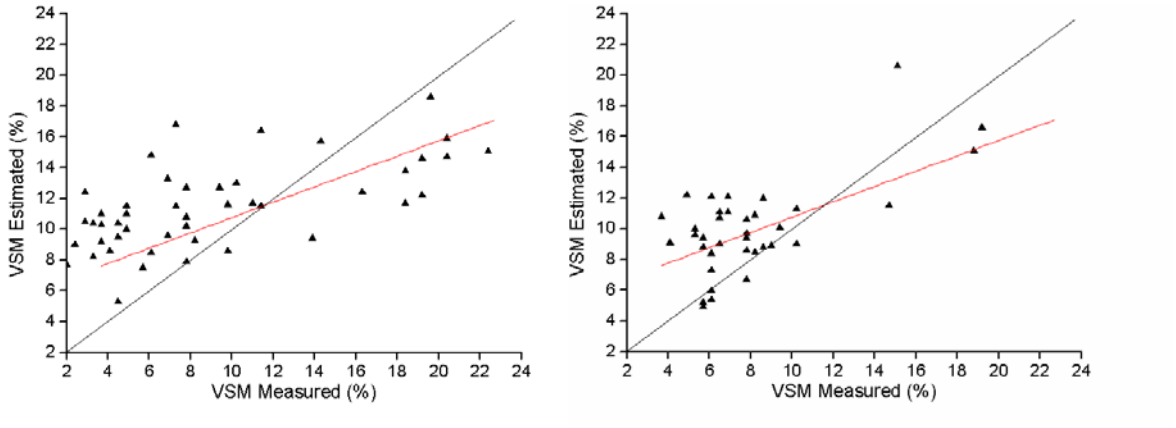

Fig. 10. Estimated VSM versus measured VSM for the Altay site (left) and the Shache site (right) over 2002-2004. The black line represents the 1:1 line and the red one represents the fit line.

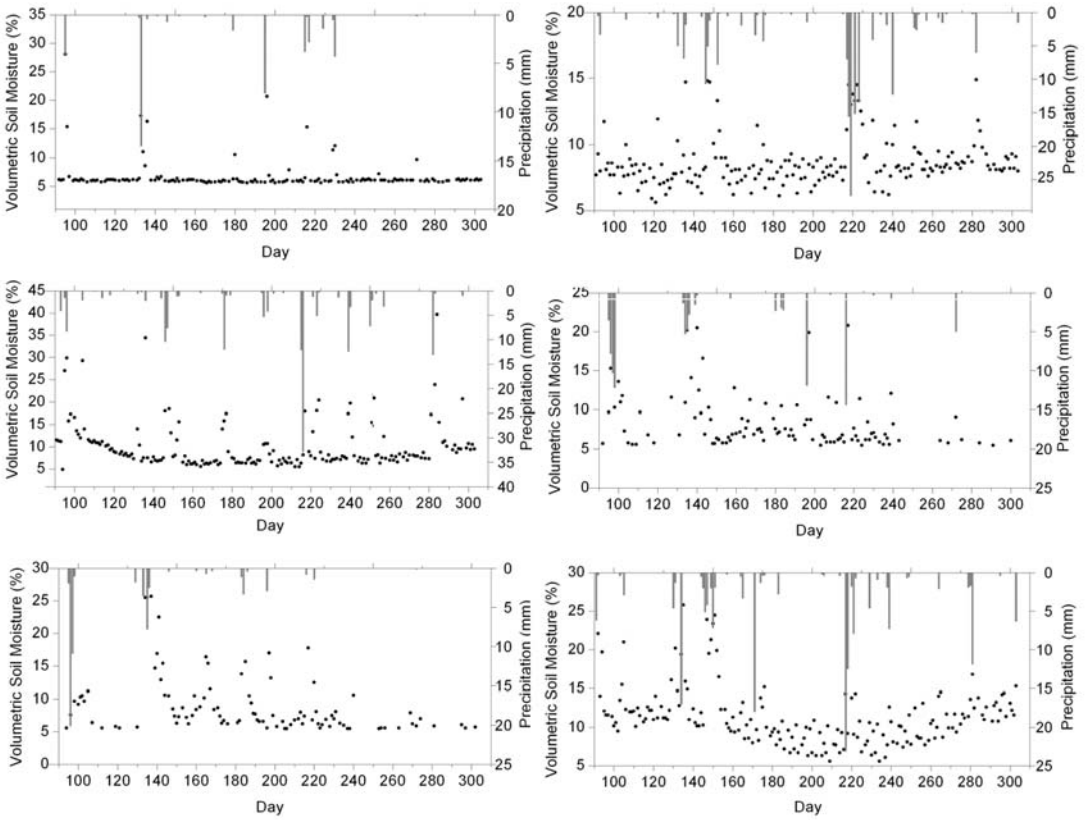

Fig. 11. Comparisons of estimated soil moisture and measured precipitation at six representative locations. Left is representative to bare soil condition (from top to bottom, corresponding to locations Tazhong, Mosuowan and Yutian), and right to vegetated soil condition (Qinghe, Hetian, and Altay)

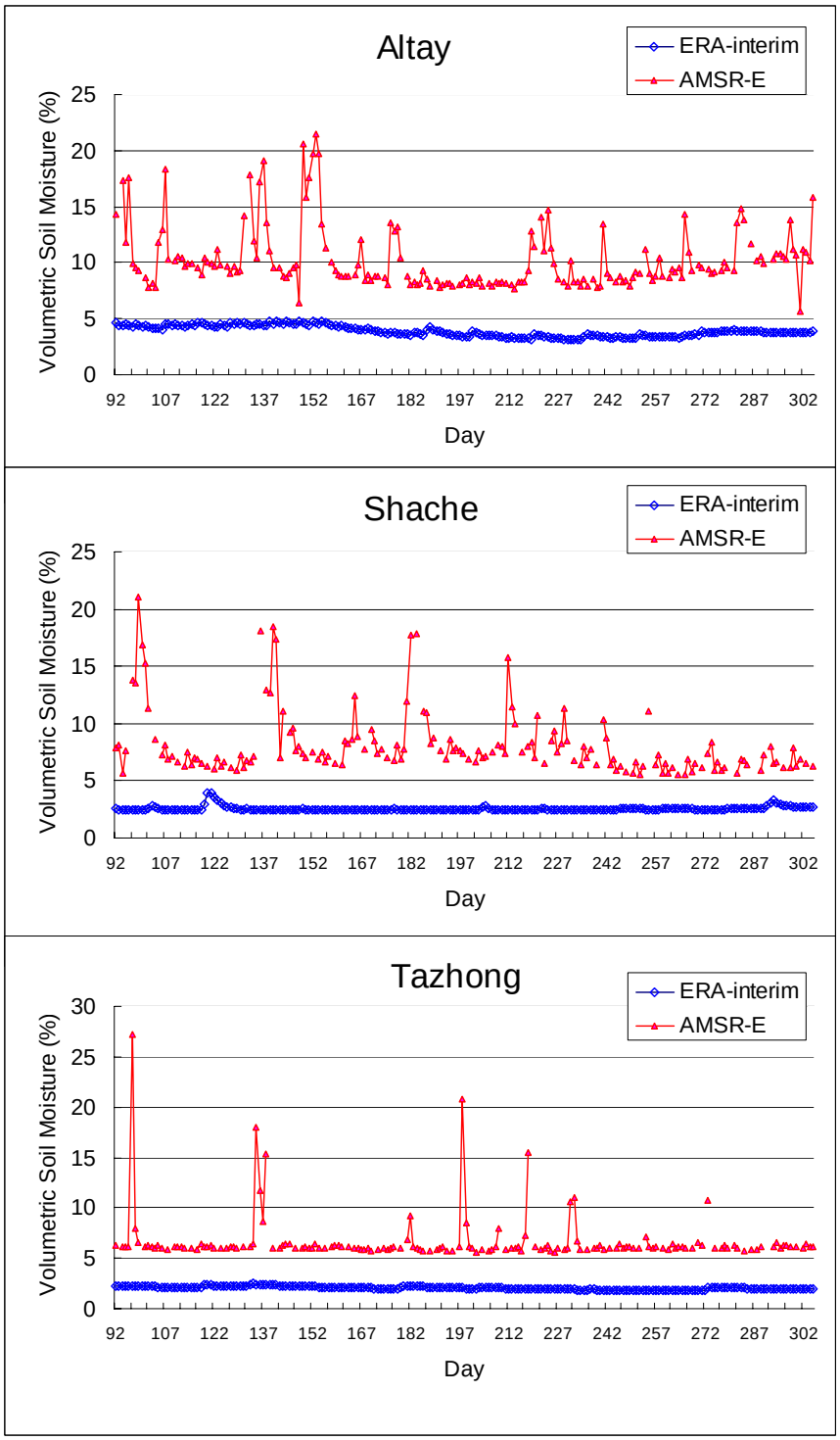

Fig.12. Comparisons of estimated soil moisture and ERA-interim volumetric soil moisture at 3 locations for the growing season (April to October) of 2004 .

Table 1. Statistics of estimated and measured VSM for the Shache site and the Altay site over 2002-2004.

Location	Mean of Estimated VSM	Mean of Measured VSM	Difference	Standard Deviation of Difference	RMSE	Correlation Coefficient Between Estimated and Measured VSM	Record Number
	(%)						
Shache	10.1	8.3	1.8	3.02	3.5	0.649	37
Altay	11.5	9.3	2.2	2.79	5.4	0.604	48